Journal of Materials and Environmental Sciences
ISSN : 2028-2508
CODEN : JMESCN

J. Mater. Environ. Sci., 2018, Volume 9, Issue 4, Page 1128-1139

https://doi.org/10.26872/jmes.2018.9.4.124

http://www.jmaterenvironsci.com

Experimental study of raw material from Moroccan oil shale and coal waste and their reuse in cement industry

S. Chhaiba[1,2*], M.T. Blanco-Varela[1] , A. Diouri[2], A. Boukhari[2]

1. Instituto de Ciencias de la Construcción Eduardo Torroja (IETcc-CSIC), C/Serrano Galvache 4, 28033 Madrid, Spain
2.Laboratory of Applied Solid Chemistry, Faculty of Science, Mohammed V University, Rabat, Morocco

Received 23 Mar 2017,
Revised 14 Dec 2017,
Accepted 17 Dec 2017

Keywords

- ✓ Oil shale LayersCoal waste,
- ✓ Burnt Oil shale,
- ✓ Pozzolanic activity,
- ✓ hydraulic material,
- ✓ Cement manufacturing,

salmachhaiba@gmail.com,
Phone: (+212)629939554

Abstract

This study aims to characterize four geological layers (T, Y, X, M) of Moroccan Timahdit's Oil shale and of Jerada coal waste to evaluate their suitability as alternative materials for cement manufacturing. Mineralogical and chemical characterizations of these materials in a raw state, and at different heat treatment's temperature, were carried out by various methods: X-ray fluorescence, X-ray diffraction, infrared spectroscopy and thermogravimetric analysis (DSC/TGA). The DSC/TGA analysis confirmed the presence of organic matter in oil shale with a combustion heats between 3459 J/g (layer M) and 5368 J/g (layer Y), while coal waste has less heat power with 889.2 J/g. Chemical and mineralogical composition of the studied materials and their thermal behavior indicate that these materials would be energetically beneficial in the production process of Portland clinker if they are used as alternative fuel. In addition, residues after oil shale layers burning can be used as pozzolan or hydraulic materials in cement, since they have shown a good activity.

1. Introduction

Oil shale is considered one of the largest energy resources in the world [1]; it may be defined as natural rocks consisting of organic and inorganic parts[2].The organic part burns to give its calorific value, the inorganic part is composed mainly of clay minerals, quartz, calcite, dolomite and carbonates used in different materials production. Oil-shale deposits have been discovered in ten regions in Morocco. The two deposits that have been studied the most are Timahdit's and Tarfaya's deposits; around 69000 examinations have been made from 157 boreholes totaling 34.632 m in length and from 800 m of mine workings. They represent about 15% of known oil shale resources in the world [3]. The thickness of the TImahdit oil shale ranges from 80 to 170 m [4]. It is subdivided into 4 lithological zones (T, Y, X and M) which contain variable organic matter content (15-20% of CO per layer) in an environment of basalt, limestone and marl [5].The major part of the oil shale is calcium carbonate besides clay minerals and some quartz.

The deposit consists of two different basins: the Northwest basin called the syncline El Koubbat and the Southeast basin called Angueur separated by the anticline Jebel Hayane [6].

On the other hand, it is known that following the decline of fossil fuels, coal continues to be widely used. Unfortunately coal production is accompanied by large amounts of estimated between 15 and 20% solid waste [7], [8]. Coal wastes are the low-energy-value discards of the coal mining industry, then, many of the heavy metals released in the mining and burning of coal are environmentally and biologically toxic elements, stored in federally unregulated coal waste sites. In the northeast of Morocco, coal exploited in the mine of Jerada was accompanied by large quantities of waste[9], [10], knowing that Morocco is experiencing a real difficulty in terms of waste recycling and recovery. Valorization of these valuable products is a great way of reducing the accumulation of large amounts of coal waste, solving urban planning problems, as well as countering environmental hazards due to the presence of high concentrations of sulfates in the groundwater as a result of the oxidation of pyrite present in these wastes [11].

At the same time, Portland cement manufacture involve a large environmental impact that has prompted the industry to implement a number of strategies geared to reducing greenhouse gas, particularly CO_2, emissions while lowering energy and natural raw material consumption. While reducing greenhouse gas, particularly CO_2

emissions. The use of alternatives fuels, secondary cementitious materials (SCMs, often industrial by-products), improvements in combustion, heat exchange and grinding technologies along with grinding additives, have diminished both emissions and consumption with no detriment to binder properties [12,13,14 and 15].
The present paper aims to characterize Moroccan oil shale and coal waste, using different methods such as X-ray diffraction, X-ray fluorescence and Infra-Red spectroscopy and to evaluate different ways for this material to be used in cement production. To investigate the possibility of oil shale's energetic contribution, we carried out a thermal investigation using differential scanning calorimetry (DSC/ TG).

2. Materials and methods

2.1. Samples origine

The samples used in this study were obtained from the Timahdit deposit that is situated in the Middle Atlas region in the north part of Morocco, 250-km southeast of Rabat and occurs in two northeast southwest trending geosynclines, the thickness of the 4 lithological zones (T, Y, X and M) in this deposit varies from100 to 150 m [6]. The considered sample of coal waste is a mixture of representative soil samples collected from different places on the embankment, from Jerada, and it is called coal waste and noted CW.

2.2. Burnt oil shale preparation

The four oil shale samples were grinded under 45 µm, and then they were characterized by XRD, FTIR, XFR and DSC/TG.
Samples from each layer were prepared to study the pozzolanic activity. The samples were shaped into pellets, and then they were introduced in platinum crucibles and calcinated at 1350 °C for 30 minutes in a laboratory furnace and then, quenched. The ashes obtained were grinded under 45 µm and characterized by XRD as well as FTIR and their free lime content was determined as specified by the Spanish standard UNE 80-243-86.
The pozzolanic activity of oil shale layers was studied chemically using an accelerated method. This method consists of contacting 1 g of sample with a saturated lime solution at a temperature of 40 °C, and kept in contact with the solution for 1 day, 8 days, 14 days and 28 days. After these periods, the solutions were filtered and then titrated with HCl (0.1 N) and EDTA (0.01785 M), using methyl orange as an indicator in order to determine their residual CaO content. The concentration of lime that has set in the samples is calculated as the difference between the initial (17.68 mmol/l) and the final lime concentration determined by titration. The main advantage of this method is that it allows us to evaluate the pozzolanic activity of the sample, without the need of making mixtures with cement, thus the activity is assessed by simple titration.
In order to identify the possible reaction products of pozzolanic or hydraulic reaction,0.2 g of oil shale M layer was mixed with 0.2 g of Portlandite and water at 40°C and was left to stand for 2 weeks; the sample obtained was dried at 40 °C for 1 hour and characterized by FTIR.

2.3. Analytical techniques

The chemical composition of Oil shale layers and coal waste samples was determined using the X-ray fluorescence, in a spectrophotometer Philips PW1404 X-Ray tube Sc-Mo, software Super-Q four analyser crystals: PX-1 GE, LIF200 and working conditions were 40KV and 70mA.Loss on ignition of the prepared Oil-shale (OS) was determined by heating it at 1000 °C, for 1 h, and the difference in weight was recorded. Mineralogical characterization of the samples was carried out with Bruker D8 Advance model X-ray diffractometer using the following measurement conditions: Voltage generator (40 kV), Current generator (30 mA) Divergence slit (variable 6 mm) Time/Step (0.5 s), Step size (0.019746 º), Scan time (23´ 47 ´´), 2theta (5 - 60 º). FTIR spectra assays were performed on a Thermo Scientific Nicolet 600 spectrometer using the KBr pellet method (0,1 mg of sample / 300 mg KBr) at frequencies ranging from 4000 to 400 cm^{-1} and a spectral resolution of 4 cm^{-1}. Differential Scanning Calorimetry analysis (DSC) and thermos-gravimetric analysis (TG) were performed using DSC/TG type SDTQ 600 with a heating rate of 10°C/min up to 1000°C, and using 100ml/min of dry air free of CO_2 as carrier gas. Finally, the BET specific surface area was determined with nitrogen adsorption isotherms.

3. Results and Discussion

3.1. Timahdit's Oil Shale Characterization

3.1.1 Raw oil shale

The chemical composition of the four layers of oil shale samples is shown in Table 1. The four layers of oil shale samples contain significant amounts of SiO_2, CaO and Al_2O_3, which are major components of Portland cement, whereas the contents of other metal oxides were less than 5 %. Accordingly, their potential use in the cement industry can be considered.

Table 1: Chemical composition (wt. %) of the four Timahdit's oil shale samples

Oxides	CaO	Al_2O_3	SiO_2	Fe_2O_3	S	MgO	K_2O	MnO	P_2O_5	LOI
OST	5.14	15.46	37.39	4.91	0.94	1.50	1.25	0.05	0.59	31.73
OSY	20.50	7.81	22.71	2.48	1.60	2.02	1.09	0.05	1.58	39.33
OSX	26.11	5.13	16.80	1.66	1.84	2.63	1.03	0.06	1.28	42.68
OSM	22.11	8.15	25.10	2.40	1.18	2.20	1.12	0.03	1.14	35.69

Figure 1 shows the diffractograms of the four layers. The major crystalline phases present in the four lithological zones (T, Y, X and M) of Timahdit deposit are calcite, quartz, dolomite, followed by kaolinite, muscovite and ankerite. We can see that the most intense reflections are due to the calcite followed by quartz and dolomite. Sample T contains less calcite and is less crystalline than the other ones, being the background of its XRD pattern more intense than the background showed by the patterns of the other layers. The kaolinite peaks appeared in the XRD pattern for the oil shale M and T samples while they are almost absent in the other layers. Additionally, the four layers contain muscovite.
Moreover, no crystalline sulfate phase was identified in spite of all samples contain sulfur; it means that sulfur measured by XRF must be associated to the organic matter which is not detected by XRD.

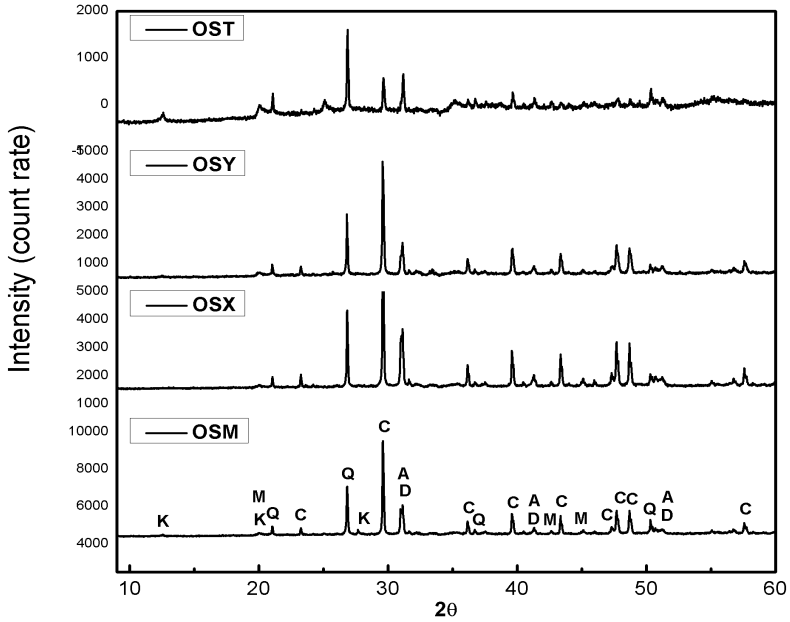

Figure 1: X-ray diffraction patterns of the raw four layers oil shale: C= Calcite, Q= Quartz, D= Dolomite, A= Ankerite, K= Kaolinite, M= Muscovite.

The oil shale layers were also characterized by infrared spectroscopy. The curves of FTIR obtained are illustrated in Figure 2. The complete interpretation of the absorption bands in measured IR spectra is summarized in Table 2. Kaolinite shows a sequence characteristic IR absorption. The two weak bands, whose sharp peaks are well defined, at 3697 cm^{-1}, 3620 cm^{-1}areassigned to OH stretching of kaolinite while the band at 3624 cm^{-1} is assigned to that vibration from muscovite. The weak band observed at approximately 914 cm^{-1} for kaolinite is a result of Al-OH bending vibrations. The band at 694 cm^{-1} is assigned to quartz and kaolinite. The doublet medium bands observed at 800cm^{-1} and 780 cm^{-1} are associated to Si–O symmetrical stretching vibration assigned to quartz. An asymmetric intense band which appears at 1034 $cm^{-1}$with three shoulders at 1014 $cm^{-1}$and 1097$cm^{-1}$and 1160 cm^{-1}areattributed to Si-O anti symmetric stretching vibration characteristic of Kaolinite and muscovite (at 1023 cm^{-1}) which are overlapped with those characteristic of quartz at 1080 and 1165cm^{-1}.Absorption bands about 1798 cm^{-1}, 1429 cm^{-1}, 875 cm^{-1} and 712 cm^{-1} are characteristic of calcite. The C-O asymmetric stretching band of calcite at 1429 cm^{-1} has a shoulder at about 1450 cm^{-1} that is related to dolomite. Additionally, bands in the range 400-570 cm^{-1} can be assigned to quartz at 512 $cm^{-1}$and 470cm^{-1};

kaolinite at 539 cm^{-1}, 471 cm^{-1} and 431 cm^{-1} and muscovite at 557 cm^{-1}, 531 cm^{-1} and 477 cm^{-1}. Finally, the spectrum consists of stretching vibration at 2923cm^{-1}assigned to the aliphatic groups of organic matter and bending vibration at 2852 cm^{-1} from aromatic groups of organic matter, which indicates that a significant amount of organic compounds is present in the Timahdit's oil shale. Those results given by FTIR confirm the presence of all crystalline minerals found by X-ray diffraction. It can be drawn from these observations that the major difference in all the spectra obtained is that the bands of kaolinite are less intense in the layers X and Y, while these bands are intense for layers M and T. It can also be observed that the bands characteristic of calcite are almost absent for the layer T except the one at 1429 cm^{-1} which is present with a low intensity.

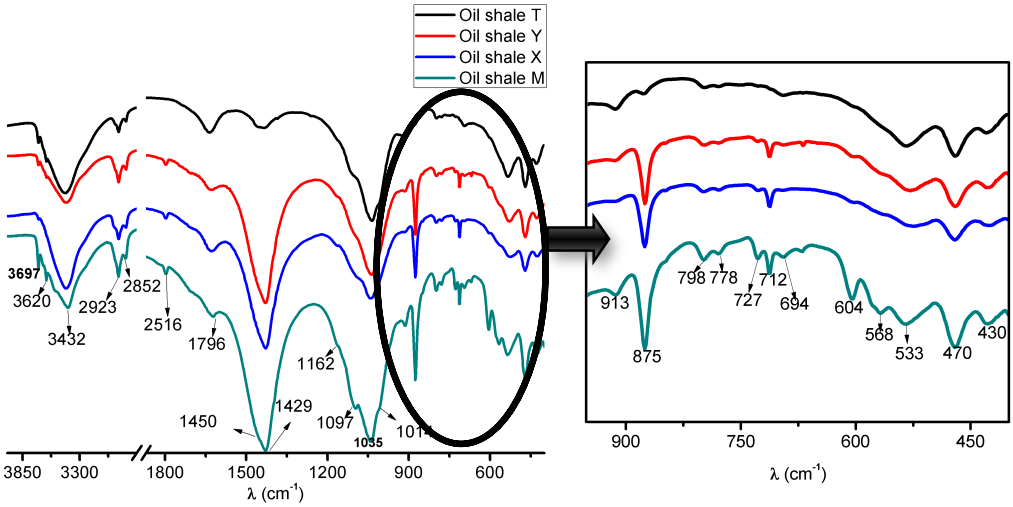

Figure 2: Oil shale layers FTIR spectra.

Table 2: Position and assignment of the absorption bands in IR spectra of oil shale

Wavenumber (cm-1)	Assignation	References
3697 - 3620 3432 - 1629	OH stretching of inner hydroxyl groups H-O streaching vibration of water	[25], [26]
2923 - 2852	C-H stretching	[27]
1627	H-O-H bending vibration of water	
1429	v3 C−O very strong symetrique vibration	[28]
1097 - 1035	Si-O very strong anti-symetric stretching vibration in silicates	[29][25], [26]
914	Al-OH bending vibrations	[30]
875	v2 C−O deformation	[28]
800 - 780	v1 Si–O symmetrical stretching vibration	[29], [31]
712	v4 C−O deformation	[28]
535 - 480	Si-O-Al stretching	
470 430	Si-O-Si bending Si-O deformation	[30], [31]

The DSC/TG study of the four Timahdit's layers oil shale yielded findings of technological interest. According to these results present in Figure 3 and Table 3, the curves could be divided into three basic stages as follows:
Stage I: Below 150 °C, a slight endothermic reaction in atmospheric pressure conditions was observed. The mass loss can be mainly attributed to the evaporation of water, especially adsorbed water from clay minerals, which accounts for almost 7 %, 2.65 %, 1.6 % and 2.36 % of total sample mass for OST, OSY, OSX and OSM

respectively. The total heat of each sample in this range is 212.6 J/g, 70.35 J/g, 47.76 J/g and 76.32 J/g for OST, OSY, OSX and OSM respectively. OST shows the highest total heat, which suggests that it contains the most water molecules:

Stage II: In a temperature range from 200 °C to 600 °C, two main exothermic reactions took place and a significant mass loss was observed; 17.88 % of total sample mass for OST, 20.65 % of total sample mass for OSY; 19.2 % of total sample mass for OSX and 14.59 % of total sample mass for OSM which could be explained by the loss of hydrocarbon material. This stage mainly involves the combustion of bitumen and kerogen into volatiles. The first peak is due to the oxidation of a portion of the volatile matter and the second is due to the oxidation of the carbonaceous residue (fixed carbon) [16]. The entire process is exothermic and the reaction is rapid and produces carbon oxides and water [17]. Whether the decomposition is single-stage or two-stage depends on the type of oil-shale [18]. The total heat here for OST, OSY, OSX and OSM respectively is 3802 J/g, 5368 J/g, 5061 J/g and 3459 J/g. The mass loss during the first combustion peak is lower (44 - 56 %) than the mass loss along the second one while the heat flow is higher (6 – 36 %) which means that the volatile fraction of the organic matter has more elevated calorific power. In this range, also kaolinite loses the hydroxyl groups, being that an endothermal reaction.

Stage III: Above 600 °C, the reaction is endothermic under air atmosphere and a last important mass loss was observed; 4.06 wt% for OST, 16.52 wt% for OSY, 21.24 wt% for OSX and 18.82 wt% for OSM. This stage is governed by the thermal decomposition of carbonates calcite and dolomite[19].Here again the total heat of each sample is 160 J/g, 478.9 J/g, 750.46J/g and 450.9 J/ for OST, OSY, OSX and OSM respectively. The decomposition of calcite in OST is less than the other ones due to the poor amount of calcite contained in this layer, whereas, the major mass loss for OSX and OSM was observed in the third stage, due to the thermal decomposition of carbonates, which can be assumed to be essentially calcite (CaCO3) and in minor proportion of dolomite ($CaMg(CO_3)_2$), that resulted in giving lime (CaO and MgO) and carbon dioxide (CO_2).

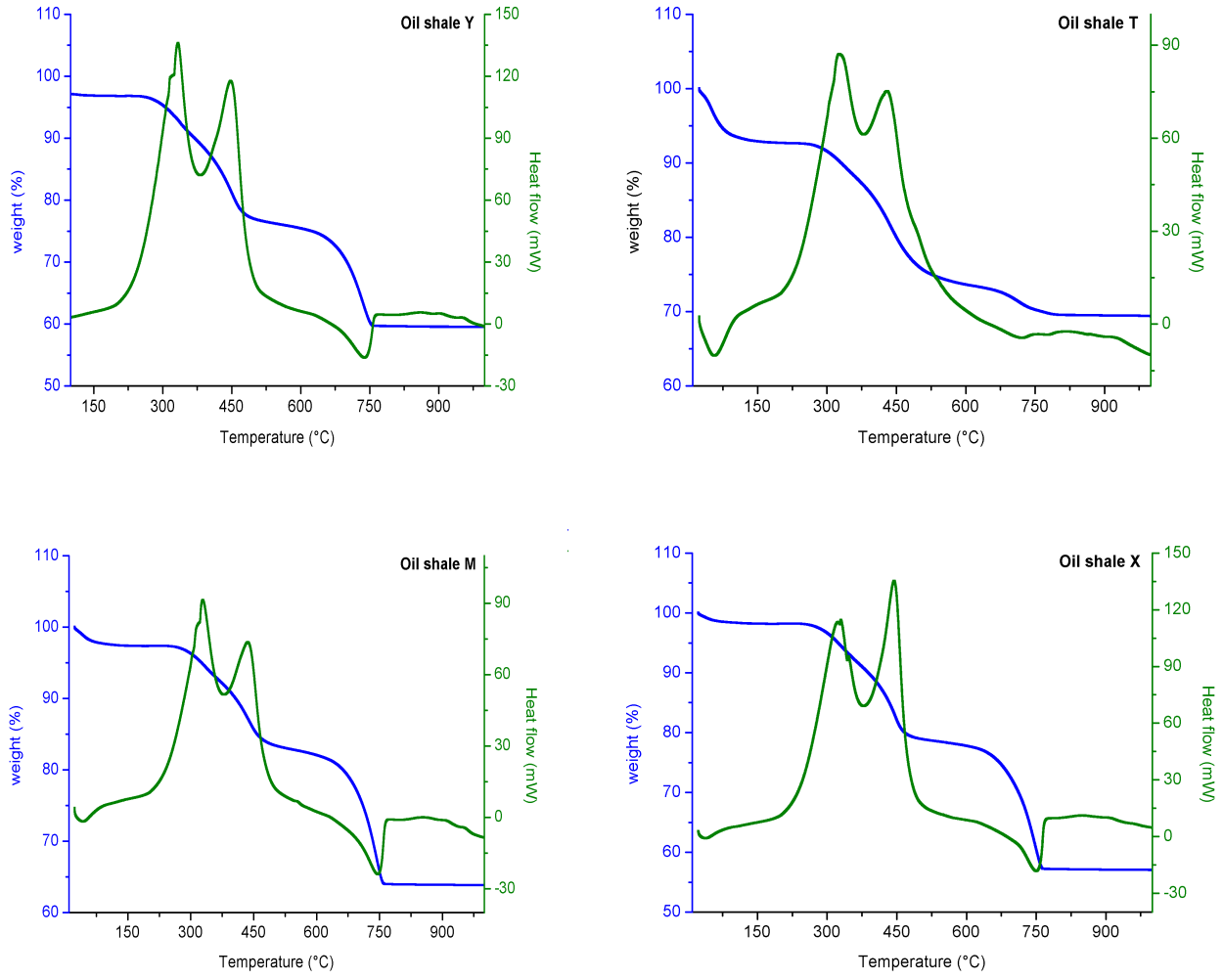

Figure 3: DSC/TGA curves of oil shale T, Y, X and M under air atmosphere-heating at 10°C min-1

Table 3: The heat flow and mass loss of oil shale T = OST; oil shale Y = OSY; oil shale X = OSX and oil shale M = OSM.

Samples	Steps	Temperature range (Cº)	DSC		Wheight Loss %	Total Weight Loss %
			Heat effect	Heat Flow(J/g)		
OST	Dehydration	24 – 154	Endothermic	212.6	7	30.74
	combustion	233 – 600	exothermic	3802	17.88	
	Dec. Calcite	600 – 800	Endothermic	160	4.06	
OSY	Dehydration	25 – 106	Endothermic	70.35	2.65	40.5
	combustion	220 - 550	Exothermic	5368	20.65	
	Dec. Calcite	550 - 800	Endothermic	478.9	16.52	
OSX	Dehydration	23 - 100	Endothermic	47.76	1.6	42.98
	combustion	224 - 550	Exothermic	5061	19.2	
	Dec. Calcite	600 - 800	Endothermic	750.46	21.24	
OSM	Dehydration	23 - 100	Endothermic	76.32	2.36	36.14
	combustion	228 – 539	Exothermic	3459	14.59	
	Dec. Calcite	611- 800	Endothermic	450.9	18.82	

Figure 4 shows the variation in the BET-N2 specific surface of the oil shale X, Y and M. The specific surface of sample changed a bit from one layer to the other, OSM and OSY have the higher surface areas with value of 11.81 m^2/g and 10.8 m^2/g respectively, while OSX has smaller specific surface 9.41 m^2/g.

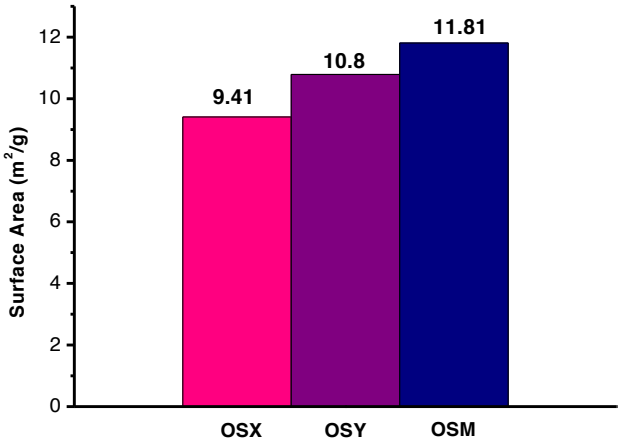

Figure 4: Variation in Oil shale Y, X and M specific surface

3.1.2. Burnt oil shale

As it was described in experimental, samples of the four oil shale layers were calcined at 1350 ºC. During thermal treatment materials melted or at least partially melted. DSC curves of the four samples showed many convergent endothermic signals in which the melting point starts at about 1200 °C (Figure 5). XRD patterns of calcined oil shale showed a very intense background and an amorphous halo at about 2θ = 29° as shown in Figure 6, no reflections due to crystalline phases were identified except those very weak in 2θ = 26° and 43° attributed to the carbon mineral. Free lime values of these samples are: OST= 0.36 wt%; OSY= 0. 28 wt%; OSX= 0. 29 wt%; OSM= 0.29 wt%. Given the chemical composition of oil shale layers, the product obtained from their combustion could have pozzolanic or hydraulic properties as Blast Furnace Slags material. In order to study the pozzolanic activity of these materials, an accelerated method was used, that follows the material-lime reaction over time. The pozzolanic activity results obtained are shown in Figure 7. It can be seen that after the

first 14 day, oil shale T shows a good pozzolanic activity, since the sample was able to fix 59 wt% of the total calcium hydroxide and 74 wt% after 28 days, followed by OSY and OSM, while OSX was less pozzolanic since it doesn't show any reaction with the lime before the 14th day, and only exhibits 55 wt% of pozzolanic activity after 28 days.

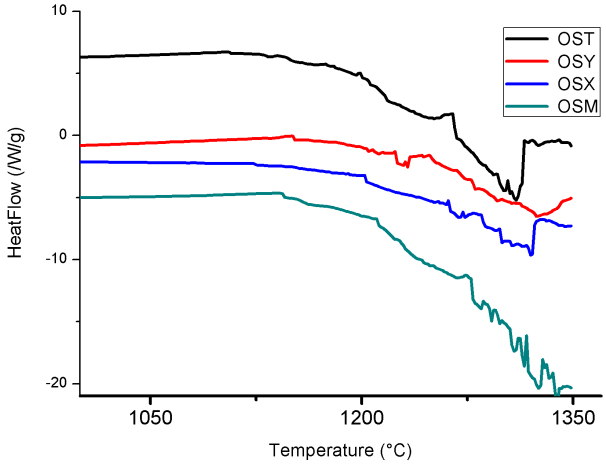

Figure 5: DSC curves of oil shale layers under air atmosphere-heating at 10 °C min^{-1}

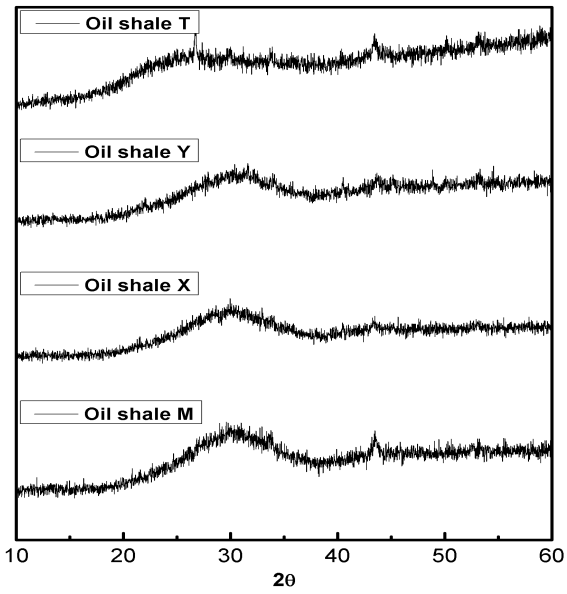

Figure 6: X-ray diffraction patterns of burnt oil shales T, Y, X and M

The product of activation of M layer with portlandite $Ca(OH)_2$ for two weeks was characterized by FTIR in Figure 8. In this figure a new band can be seen located in the range of v_3Si-O stretching asymmetric vibration at 965 cm^{-1} characteristic of C-S-H gel as a result of the activation of the sample of burnt oil shale M layer by portlandite $Ca(OH)_2$. The spectrum also contains a band at 3645 cm^{-1} due to the OH stretching vibration of $Ca(OH)_2$, v_3 and v_2C-O bands respectively at 1421–1482 cm^{-1} and 875 cm^{-1} due to the presence of calcium carbonate resulting from the reactions of atmospheric CO_2 with calcium hydroxide. We can conclude that OSM layer can be considered as a hydraulic material that is able to be activated by the presence of portlandite producing C-S-H gel while it does not seem to consume important amounts of portlandite during the pozzolanic test. To explore the use of new fuels or new raw material in cement production is an increasingly common industry practice that allows a more rational and environmental friendly use of natural resources and wastes. In cement manufacturing, there are three possibilities of using oil shale: Either use it directly at the kiln following the same circuit as alternative fuel, or as prime materials to elaborate raw meal to be clinkerized, or after combustion, the ash obtained in a thermal power plant could be used as an addition to the clinker.

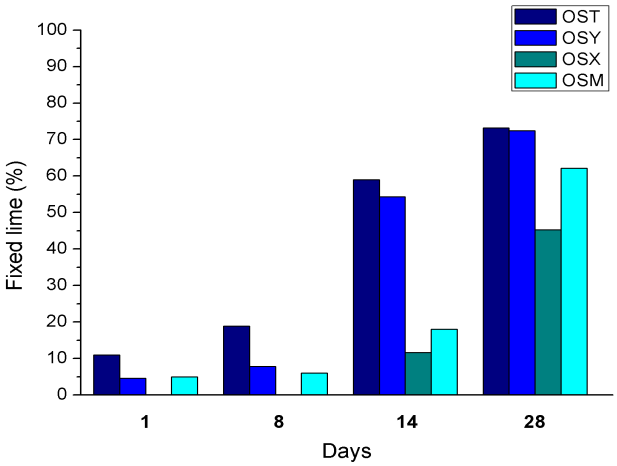

Figure 7: Pozzolanic activity: fixed lime over time of burnt oil shale layers

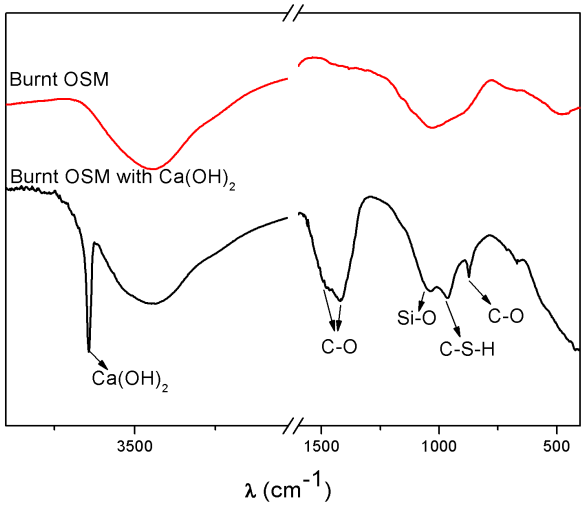

Figure 8: Activated burnt oil shale M FTIR spectrum.

The studied oil shales contain a variable percentage of hydrocarbons (14 to 20 wt%), depending on the lithological layer which are extracted, the combustion occurs between 200 and 550 °C and the heat output being between 3450 and 5350 kJ/kg . Alternative fuels generally used in the main cement furnace burner have at least a heat power of 6000 kJ/kg, so this type of materials could be used partially replacing the fuel in the precalcinator. According to the experience of Hilger [21], incorporating oil shales of poor quality (3400 Kj/kg, similar to those of the T and M Timahdit layers), finely ground directly into the precalcinator contributes to 20% of energy and 10 wt% of the raw material in the clinkering process. In the case of the oil shale studied, from layers Y and X, the energy input could be 30 %.

Given the chemical and mineralogical composition of the inorganic fraction of the four layers of the studied oil shale, other use could be as a prime material in the manufacture of cement raw meals. Organic matter of these materials combusts in two stages, first the most volatile, then the heavier material, and both of these reactions occur above 200 °C, so that the combustion would not be produced during grinding of raw meal and there would not have risk of combustion or explosion during this stage of the cement production. In this case the combustion would occur in the preheater before reaching the furnace, providing energy in this stage.

At the same time, the use of ashes of the calcination of oil shales in power stations as component of cements depends on the initial chemical and the final mineralogical compositions. During the combustion process, in addition to the oxidation of organic matter and sulfur, thermal decomposition reactions occur where clay loses its constitutional water and limestone, whereas calcium and magnesium lose their CO_2, leaving CaO or MgO as residue. Once limestone is decarbonated, solid state reactions between acids, oxides (SiO_2, Al_2O_3, and Fe_2O_3) and bases (CaO and MgO) will begin to occur forming calcium or magnesium salts. Thus, the degree of the achieved combination and consequently the mineralogical composition of the obtained ash vary depending on the fineness of the material, the temperature reached in the process, the residence time of the material in the

boiler, the type of boiler and dust collector system used as well as the chemical composition of the oil shale. Calcined oil shale is at present a component of common cements (EN 197-1:2011), the norm suppose that it has hydraulic properties and establishes the required values of compressive strength and expansion of mortars elaborated with this material.

Raado and Nurm [22] reported the mineralogical and chemical composition of burnt oil shales, obtained at temperature higher than 1300 °C in a pulverized fuel combustion boiler, which contains 9 % of free lime while the other from fluidized bed boiler (low combustion temperature, 800 °C), contained 6 % of CaO. It is known that free lime and periclase are dangerous phases for volume stability of concrete given its slow hydration rate and the expansive character of that hydration, so this material would be classified as secondary cementitious material (T in the norm EN-197-1), if it satisfies the mechanical and volume stability requirements stablish in such a Norm. However the free lime content of the four burned oil shale layers yield under 0.5 wt% which ensure no expansive problems during hydration of blended cements when the mentioned ashes were used as addition to clinker. Burned OST layer material cannot have hydraulic properties because it does not contain enough calcium, however it exhibited a good pozzolanic characteristic, which indicates that it could be used as pozzolanic additional minority component of cement (< 5 wt%) or as addition to concrete.

Burned M, X,Y layer materials do not contain hydraulic phases similar to the ones of clinker, as described in EN 197-1:2011, they are amorphous materials of similar composition to blast furnace slag, having $(CaO+MgO)/SiO_2 \approx 1$ for M and Y, and > 1 for X layer. In order to explore the possible hydraulic capacity of these layers, a sample of M layer was activated with portlandite and submitted to an accelerated pozzolanic test; results demonstrated its hydraulic character producing a large amount of C-S-H gel after only 2 weeks while it did not consume important amounts of CaO during the pozzolanic test.

3.1.2. Characterization of Jerada Coal waste

The chemical composition of the CW, obtained with XRF is given in Table 4. According to the mineralogical analysis of CW and the results of Rietveld quantitative XRD mineralogical analysis of their crystalline phases, we can notice a high proportion of quartz 65.5 %.The remaining crystalline phases present in CW are muscovite, illite, clinochlore and gypsum in minor proportion as seen in Figure 9 and Table 5.

Table 4: Chemical composition (wt. %) of CW

Oxides	CaO	Al_2O_3	SiO_2	Fe_2O_3	SO_3	MgO	K_2O	MnO	P_2O_5	LOI
CW	0.56	21.59	52.18	4.663	0.97	0.99	2.95	0.077	0.08	14.22

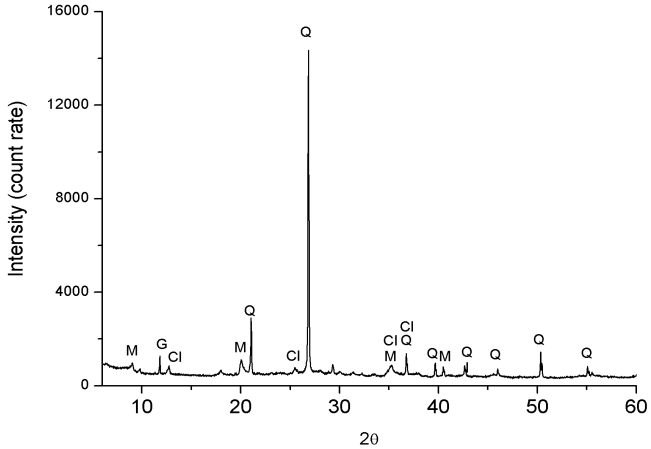

Figure 9:X-ray diffraction patterns for CW with different granulometry. Q= quartz; M = Muscovite; G= gypsum; Cl= Clinochlore

The FTIR spectrum of CW is shown in Figure 10, the complete interpretation of the absorption bands in measured IR spectra is summarized in Table 6. The spectrum presents in the range of O-H stretching vibrations an acute and weak band at 3620 cm^{-1}coupled with the 829 cm^{-1} and 750 cm^{-1} doublet which indicate muscovite and illite. The (Al-Al-OH) and (Al-Mg-OH) deformation bands of illite are respectively situated at 916 and 833 cm^{-1} and Al-Mg-OH deformation band characteristic of muscovite is located at 1026 cm^{-1}. The medium intensity broad band,at 3431 cm^{-1} is due to water. In the Si-O stretching vibrations region it is shown a broad and intense band where overlapping vibrations from quartz at1170 cm^{-1} and 1082 cm^{-1}, clinochlore appears at 988 cm^{-1} due

to the Si-O stretching vibration. Also, we can see a doublet at 798 cm^{-1} and 778 cm^{-1} due to Si-O symmetrical stretching vibrations of quartz and medium intensity bands O-Si-O deformation at 536 $cm^{-1}$and 476 cm^{-1} of muscovite, illite and quartz.

Table 5: the original CW mineralogy (% by weight) obtained by Rietveld refinement

Chemical formula	Name	Content (Rietveld) %
SiO_2	Quartz	60.29
$KAl_2(AlSi_3O_{10})(OH,F)_2$	Muscovite	10.12
$(K,H_3O)Al_2$ $Si3AlO_{10}(OH)_2$	Illite	19.2
$(MgAlFe)_6(Si,Al)_4O_{10}(OH)_8$	Clinochlore	6.8
$CaSO_4 \cdot 2H_2O$	Gypsum	3.5

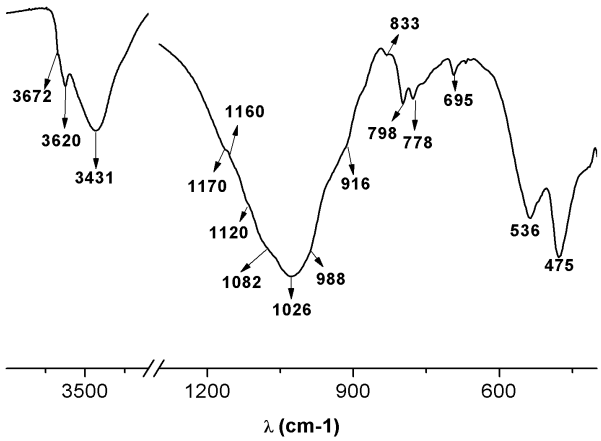

Figure10: Coal waste FTIR spectra.

Table 6: Position and assignment of the absorption bands in IR spectra of CW

Wavenumber (cm^{-1})	Attribution	References
3672	Stretching OH vibration (shoulder) of illite	
3620	Stretching OH vibration of muscovite + illite	
3431	Broad band of medium intensity: stretching OH vibration of water.	
1160 -1070	Very strong intensity band antisymmetric Si-O vibration of Quartz	
1028	Very strong intensity band antisymmetric Si-O vibration of muscovite and illite	
988	Very strong intensity band antisymmetric Si-O vibration of clinochlore	[20], [32]
916	Weak intensity overlapped band Al-Al-OH deformation of muscovite and illite	
833	Weak intensity band Al-Mg-OH deformation of muscovite and illite	
798-778	Medium intensity bands Si-O symmetric stretching of quartz.	
694	Weak intensity band of O-Si-O symmetrical bending vibration of quartz.	
536-476	Medium intensity bands O-Si-O deformation of muscovite and illite.	

Results for the analysis of CW by TG/DSC in air atmospheres are given in Figure 11 and Table 7. Many chemical and physical processes contribute to the observed mass loss.

In the temperature range 20-650 °C, we notice two basic stages that are included as follows:

- A first endothermic region: between 23 and 150 °C, attributed to the evaporation of free and bounded water [20] with a heat flow of 92.66 J/g.
- An exothermic region between 300 and 650 °C attributed to the combustion of the organic fraction in the samples of coal waste and also overlapped with an endothermic peak of clinochlore, with 889.2 J/g of total heat**.** At that temperature, only one step of combustion is observed for pure coal. Only 12.3 % of the total mass was

lost during this treatment which means that there is a 3.87 % weight loss during the first endothermic region and a 7.3 % weight loss for the exothermic region.

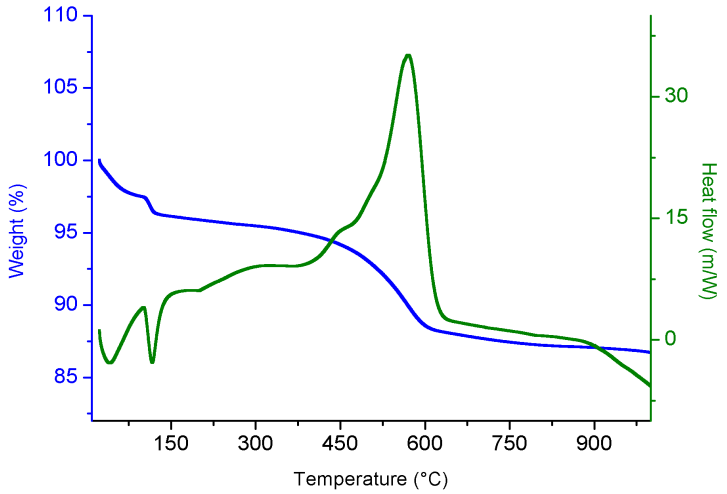

Figure 11: DSC/TGA curves of CW under air atmosphere-heating at 10 °C min^{-1}

The chemical composition comparison of oil shale and coal waste revealed that the main difference among of these materials is calcium oxide and quartz, where the four layers of oil shale contain more CaO, and CW contains more SiO_2 (Table 1 and Table 4).The major crystalline phase in the four layers of oil shale was calcite along with quartz, dolomite, kaolinite, muscovite and ankerite, while quartz was the most abundant crystalline phase in coal waste followed by chlinoclore, muscuvite and illite.

Table 7: The heat flow and mass loss of CW

Steps	Temperature range (ºC)	Mass loss %	Total loss %	DSC	
				Heate ffect	Heat Flow (J/g)
Dehydration	23 - 154	3.88	12.3	Endothermic	93
Combustion	313 - 652	7.76		Exothermic	891

The presence of all those crystalline phases may suggest that clay can be substituted and that limestone can be partially replaced by oil shale in cement manufacturing while coal waste can only be used as clay/quartz substitute in the elaboration of raw meal of cement. Furthermore, the DSC/TG results, up to 600°C, have shown that the weight loss was more significant for the four layers of oil shale than coal waste. Since at that temperature, all the organic matter burns off, this amount of organic matter can be appropriated to provide part of the energy required to make Portland cement [23], also it would reduce fossil fuel consumption in a modern cement kiln [24]. While at temperatures between 600 and 800 °C, an important mass loss was observed due to the decomposition of carbonates present in the four layers of oil shale. The CO_2 produced was 14.17 wt% which corresponds to 32.20 wt% of $CaCO_3$ in sample, according to the following reaction: $CaCO_3 \rightarrow CaO\ (s) + CO_2\ (g)$. However, those carbonate are not present in CW. The main difference observed between the four layers and CW was in the third stage of thermal decomposition in which the loss weight and the heat flow is very weak due to the lesser amount of calcite contained in this sample as confirmed by FTIR analysis.

4. Conclusions

Several environmental issues occur with the use of oil shale for production of shale oil by pyrolysis**.** Similarly the coal waste is also hazardous to environment. Taking into consideration these problems, the use of these materials in the cement industry for production of Portland cement is a great alternative. This study was focused into evaluating this possibility, to valorize these materials and to consider a greener use for them. The main conclusions are:

1. The four layers from Thimahdit oil shale have a suitable chemical composition and enough calorific power to be used as fuel in the precalcinator of cement kilns. The studied coal waste has less calorific power and consequently is less adequate to this use.

2. The studied four layers could be used as prime materials in the elaboration of raw meal mixes of cement, substituting to clays and partially to limestone. Their combustion temperature is over 200ºC which guarantees the absence of combustion or explosions in the grinding step. Their combustion would occur inside the preheater.
3. Residues of burnt oil shale in power stations could be used as added secondary material to cement. Oil shale T layer has showed a better pozzolanic activity than X, Y and M layers, these ones showed hydraulic properties.
4. The results obtained upon this study favour the utilization of Moroccan coal waste and oil shale, as alternative materials to manufacture Portland cement clinker.

Acknowledgments-This paper has been carried out as part of a CSIC-Mohammed V University of Rabat, cooperation programm (i-COOPA20067). Facilities given by IETcc (CSIC) and funding from BIA 2013-47876-C2-1-P and BIA BIA2013-43293-R projects as well as the Regional Government of Madrid Community and European Social Fund (Geomaterials Programme2 S2013/MIT-2914) are gratefully acknowledged.

References

1. A. Y. Al-Otoom, *J. Cem. Concr. Compos*. 28 *(*2006) 3–11.
2. H. Guo , J. Lin , Y. Yang , Y. Liu, *J. Fuel*. 118 (2014) 186–193.
3. A. Sadiki, W. Kaminsky, H. Halim, O. Bekri,*J. Anal. Appl. Pyrolysis*. 70 (2003) 427–435.
4. J. R. Dyn. *Oil Shale*. 20 (2003) 193–252.
5. F. Gaboriaud , J. P. Vantelon , A. Guelzim, L. Julien ,*J. Anal. Appl. Pyrolysis.* 21 (1991) 119–131.
6. A.Saoiabi, A. Doukkali, M. Hamad, A. Zrineh, M. Ferha, Y. Debyser, *J. Comptes Rendus l'Académie des Sci. - Ser. IIC - Chem.* 4 (2001) 351–360.
7. D. Belkheiri, A. Diouri, M. Taibi, O. Sassi, J. Aride*, J. Mater. Environ. Sci.* 6 (2015) 1570–1577.
8. B. Bendra, M. Sbaa, S. Fetouani, L. A., *Int. J. Engingeering Sci. Reserach Technol.* 3 (2011) 7905–7929.
9. Y. Darmane, A. Alaoui, S. Kitane, M. Bennajah, A. Daramy, M. Cherkaoui, *Sep. Purif. Technol.* 68 (2009) 125–128.
10. D. Belkheiri, M. Taibi, A. Diouri, A. Boukhari, A. Aride, O. Sassi, *MATEC Web of Conferences 11* (2014) p. 1009.
11. Y. Taha , M. Benzaazoua, R. Hakkou , M. Mansori, *J. Miner. Eng.* DOI10.1016/j.mineng. 09 (2016) 001.
12. J.S. Damtoft, J. Lukasik, D. Herfort, D. Sorrentino, E.M. Gartner, *J. Cem. Concr. Res*. 38 (2) (2008) 115–127.
14. F. Puertas, M.T. Blanco Varela, *J. Mater Construcc*. Nº 274 (2004) 51-64.
15. N. Husillos Rodríguez, S. Martínez-Ramírez, M.T. Blanco-Varela, S. Donatello, M. Guillem, J. Puig, C. Fos, E. Larrotcha, J. Flores. *Journal of Cleaner Production*, V. 52 (2013), pp. 94–102. M.C.G
16. M. F. Martins, S. Salvador, J. F. Thovert, G. Debenest, *J. Fuel* 89 (2010) 144–151.
17. M. V. Kok, A. S. Gundogar, *J. Fuel Process. Technol.* 116 (2013) 110–115.
18. P. T. Williams, N. Ahmad *, J. Appl. Energy* . 66 (2000) 113–133.
19. F. Bai, W. Guo, X. Lü, Y. Liu, M. Guo, Q. Li, Y. Sun, *J. Fuel.* 146 *(* 2015) 111–118.
20. L.Vaculíková, E. Plevová, *J. Acta Geodyn. Geomater* 2 (2005) 167–175.
21. J. Hilger. *Oil Shale.* 20 *(* 2003) 347–355.
22. L.-M. Raado, V. Nurm, *CESB 07 PRAGUE Conference Session W1C: Materials 3* (2007).
23. M. A. Trezza, A. N. Scian, *J. Cem. Concr. Res.* 35 (2005) 438–444.
24. N. Husillos Rodriguez, S. Martinez-Ramirez, M. Teresa Blanco-Varela , S. Donatello, M. Guillem, J. Puig, C. Fos, E. Larrotcha, J. Flores, *J. Clean. Prod.* 52 (2013) 94–102.
25. L. Vaculíková, E. Plevová, S. Vallová, I. Koutník, *J. Acta Geodyn. Geomater.* 8 (2011) 59–67.
26. E. Balan, A. M. Saitta, F. Mauri, G. Calas. *Am. Mineral.* 86 (2001) 1321–1330.
27. Y. Sun, F. Bai, B. Liu, Y. Liu, M. Guo, W. Guo, Q. Wang, X. Lü, F. Yang, Y. Yang, *J. Fuel.* 115 *(* 2014) 338–346.
28. A. Kiros, A. V Gholap, G. E. Gigant. *Int. J. Phys. Sci.* 8 (2013) 109–119.
29. B. J. Saikia, G. Parthasarathy, N. C. Sarmah, *J. Bull. Mater. Sci.* 31 (2008) 775–779.
30. B. J.Saikia, G. Parthasarathy, *J. Mod. Phys.* 1 (2010) 206–210.
31. W. R. Fischer, *J. Zeitschrift für Pflanzenernährung und Bodenkd.* 140 (1977) 247–248.
32. B. Davarcioglu. *Clay Minerals in Nature - Their Characterization, Modification and Application*, InTech (2012).